



## STRUCTURAL PROPERTIES OF POLYPYRROLE - LEAD OXIDE COMPOSITES

Vidyadhara<sup>1</sup>, Smita Biradar<sup>2</sup>, Pooja Mallinath<sup>3</sup>, Rakesh Mallinath Indi<sup>4</sup>, Roopa Swaminath<sup>5</sup>

<sup>1,3,4 &5</sup>PG Studies and Research in Physics, Sharnbasva University Kalaburagi, Karnataka, India

<sup>2</sup>Bheemanna Khandre Institute of Technology, Bhalki, Bidar, Karnataka, India

Email id: [vidyadharpcj64@gmail.com](mailto:vidyadharpcj64@gmail.com)

### ABSTRACT

**Conductive Polymers:** Conductive polymers are a class of materials that combine the properties of conductive metals and insulating plastics. They have unique electrical and mechanical properties that make them promising materials for various applications.

PPy-PbO composites are a specific type of conductive polymer nano composite. These composites aim to overcome the inadequate mechanical properties of polypyrrole (PPy) while adding conductivity to lead oxide (PbO), which is one of the most abundant materials. The PPy-PbO composites are synthesized chemically using potassium permanganate or persulfate as oxidants. These chemicals are commonly used in the synthesis of conductive polymers. FTIR spectroscopy is used to analyze the bonding nature of the synthesized PPy-PbO composites. It provides information about the chemical functional groups present in the material. XRD analysis is performed to determine the presence of PbO in the polymer. XRD is a technique used to study the crystal structure of materials. This analysis is conducted to confirm the presence of lead oxide in the composite material. It helps in quantifying the elemental composition. TGA measures the change in weight of a material as a function of temperature. It is used to study the thermal stability and decomposition behaviour of the composite. SEM is used to examine the morphological characteristics of the composite samples. It provides high-resolution images of the material's surface, allowing for the observation of its microstructure. This electrical characterization technique is used to study the electrical behavior of the PPy-PbO nano composite. It measures the material's conductivity or resistivity.

These characterization techniques are essential for understanding the properties and quality of the synthesized PPy-PbO composites. They provide valuable information about the composition, structure, morphology, and electrical behavior of the material, which is crucial for assessing its suitability for various technological applications.

**Key Words:** Characterization, Composition, Lead Oxide, Nano material, Polypyrrole,

### 1. Introduction:

PPy is synthesized through the oxidation of pyrrole in organic solvents. This process results in a polymer with a positive charge on its backbone. Lead oxide (PbO) is chosen as a component for the hybrid materials due to its unique characteristics, including an oxidizer is used to improve the processibility and mechanical properties of PPy. Different compositions of the PPy/PbO composites are prepared with varying percentages



of PPy and PbO to study their structural properties, morphology, and electrical conductivity. The research focuses on the unique electrical properties of composite materials, which have gained attention in recent years. PbO is highlighted as an n-type semiconductor with good photocatalytic activity. Its electrical and optical properties are improved in one-dimensional structures. Nanosized particles are incorporated into the composites, and their high thermal stability facilitates the synthesis process. The electrochemical properties, including biocompatibility, are discussed as they play a significant role in electrical conduction and have potential applications in biosensing. Various characterization techniques are employed to study the synthesized materials, including SEM, XRD, EDS, TGA, DTA, and FTIR. These techniques provide insights into the structural and chemical properties of the composites. The interaction between PPy and PbO nano composites is investigated at different concentration levels, ranging from 10% to 50% PPy-PURE.

Overall, research project aims to investigate the structural, morphological, and electrochemical properties of PPy and its nano composites with PbO, shedding light on their potential applications in various fields due to their unique properties and characteristics.

## 2. MATERIALS AND METHOD

**Pyrrole:** Analytical reagent grade pyrrole is used, which typically indicates a high level of purity suitable for laboratory applications.

**PbO (Lead Oxide):** Analytical reagent grade PbO is also used, which means it meets specific purity and quality standards suitable for analytical and research purposes.

The purified pyrrole and PbO are stored in the dark at 40°C. Storage conditions are important to prevent degradation or contamination of the materials. Storing them in the dark helps prevent exposure to light, which can sometimes cause unwanted reactions or degradation. The in-situ polymerization method is used for the polymerization of pyrrole. In this method, the polymerization takes place within the reaction mixture itself, typically with the addition of an oxidant like potassium permanganate.

### 3 Experimental set up to Synthesis of PPy/PbO nano composite:

#### Preparation of Ethanolic Pyrrole Solution:

3 or 4 mL of distilled pyrrole is added to 25 mL of ethanol.

The mixture is stirred well for 10 minutes to ensure proper dissolution and homogenization of pyrrole in ethanol.

#### Addition of FeCl<sub>3</sub>.6H<sub>2</sub>O:

To the ethanolic pyrrole solution, 25 mL of FeCl<sub>3</sub>.6H<sub>2</sub>O is added drop by drop with continuous stirring. FeCl<sub>3</sub> acts as an oxidizing agent in the polymerization process.

The suspension is allowed to stay for complete polymerization. During this time, pyrrole monomers polymerize to form polypyrrole.

**Filtration and Washing:**

After polymerization, the suspension is filtered to separate the black precipitated polypyrrole from the reaction mixture.

The filtered polypyrrole is then thoroughly washed with distilled water. This step is essential to remove any unreacted pyrrole and excess ferric chloride.

**Drying:**

The washed polypyrrole is dried under acetone. Acetone is used to remove any residual water and facilitate the drying process.

The drying is carried out at a temperature between 60-70°C for 1 hour to ensure that the polypyrrole is completely dry.

**Preparation of PPy-PbO Nano composites:**

The dried polypyrrole is finely ground into a powder.

Different weight percentages (10%, 20%, 30%, 40%, and 50%) of PbO are added to the polypyrrole powder. The mixture of PbO and polypyrrole is stirred for 3 hours at a low temperature (0-5°C) using a magnetic stirrer. This process disperses PbO particles within the polymer matrix.

**4. Characterization Techniques:****X-Ray Diffraction (XRD) Analysis:**

Equipment: Rigaku Corporation's Smart Lab 3kW X-ray diffractometer. Operating Parameters: Voltage: 200 VAC  $\pm$  10%, Frequency: 50/60 Hz Scan Range:  $2\theta$  range of 20-70 degrees Scan Speed: 5 degrees per minute, XRD is used to analyze the crystalline structure and crystallographic properties of the PPy-PbO nanocomposites.

**Scanning Electron Microscopy (SEM):**

Equipment: Hitachi SEM model S-3400N. Made in Japan. SEM allows for the examination of the surface morphology and microstructure of the synthesized materials, providing high-resolution images. Energy Dispersive Spectroscopy (EDS), Equipment: Norman System7 by Thermo Fisher Scientific. EDS is used in conjunction with SEM to analyze the elemental composition of the materials. It can identify and quantify the elements present in the samples.

**Thermo Gravimetric Analysis and Differential Thermal Analysis:**

Equipment: STA 2500 Instrument. Heating Rate: 10°C per minute Atmosphere: Inner N<sub>2</sub> atmosphere, TGA and DTA are used to study the thermal stability and decomposition behavior of the materials under controlled heating conditions.

**Fourier Transform Infrared (FT-IR) Spectroscopy:**

Equipment: Spectrum Two spectrometer. Wave Number Range: 4000-450 cm<sup>-1</sup> FT-IR is employed to analyze the chemical bonding and functional groups present in the PPy-PbO nanocomposites. KBr disks are used to prepare the samples for FT-IR analysis.

These characterization techniques provide valuable information about the structural, morphological, elemental, thermal, and chemical properties of the PPy-PbO nanocomposites. The combination of XRD,

SEM-EDS, TGA-DTA, and FT-IR allows for a comprehensive analysis of the synthesized materials, aiding in understanding their properties and potential applications.

## 5. Result and Discussion:

### 5.1 XRD Analysis:

Figure-1 shows In the XRD pattern, there is a broad diffraction peak observed in the range of 200 to 450, which is attributed to the periodicity of the PPy chain. This peak suggests that the PPy component of the composite has a certain degree of crystallinity.

The average crystallite size of the PPy component is calculated to be approximately 3 nanometers (nm) using the Scherer formula:  $D = 0.9\lambda / \beta \cos\theta$ .

The XRD pattern of pure PPy does not show any Bragg's reflection. This suggests that the PPy is mostly amorphous in nature, lacking well-defined crystallographic planes. In contrast, the XRD pattern of the PPy-PbO composite exhibits Bragg's reflections. This indicates the development of crystallinity within the composite. The presence of PbO seems to induce crystalline order in the PPy matrix, the shifting of the XRD peaks in the composite compared to pure PPy. This shift can be attributed to the encapsulation of PbO particles within the PPy matrix, which can influence the crystallographic arrangement and spacing of PPy chains.

The XRD analysis of the PPy-PbO composites reveals that the addition of PbO leads to an increase in crystallinity within the PPy matrix. This increased crystallinity is evident from the appearance of Bragg's reflections in the composite's XRD pattern. Additionally, the shift in peaks suggests that PbO incorporation affects the arrangement of PPy chains. These findings provide valuable information about the structural changes induced by the presence of PbO in the composite, which can impact the material's properties and performance in various applications.

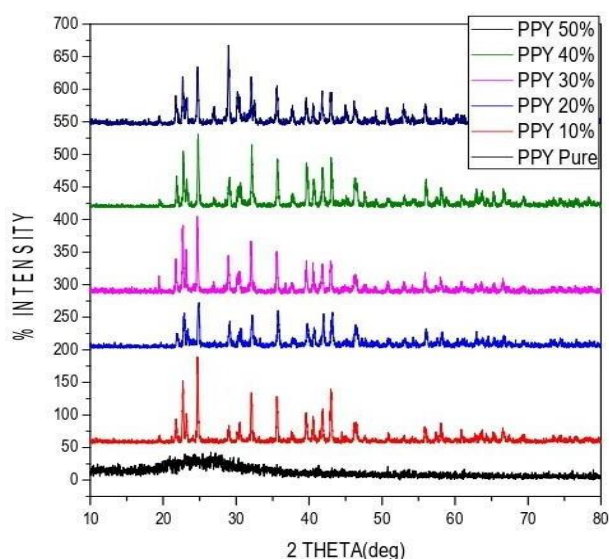


Figure-1 XRD pattern of PANI & Composite

### 5.2 Morphological Analysis SEM :

SEM images of PPy-PbO different composites with different resolution are shown in Figure 2, The micrographs show that PbO particles are completely encapsulated within the PPy matrix. This encapsulation is a crucial aspect of composite formation, as it ensures that PbO is well-dispersed within the PPy.

The SEM images reveal that the composite grains exhibit agglomeration, where multiple particles come together to form larger structures. These agglomerated grains have a spherical morphology. The average particle size of the composite grains is estimated to be around 10  $\mu\text{m}$ . This size provides an indication of the scale of the agglomerated particles in the composite.

The SEM images clearly demonstrate that the incorporation of PbO has a significant effect on the morphology of PPy. The irregularly shaped particles and their agglomeration suggest changes in the microstructure.

The average grain size of the PPy-PbO composite is calculated using the equation  $D = 1.56C/MN$ , where C is the length of the line measured in the SEM image, M is the magnification, and N is the number of intercepts.

The calculated grain size increases with the increase in the weight percentage (wt%) of PbO in the nanocomposite, indicating that the presence of PbO affects the grain size of the composite.

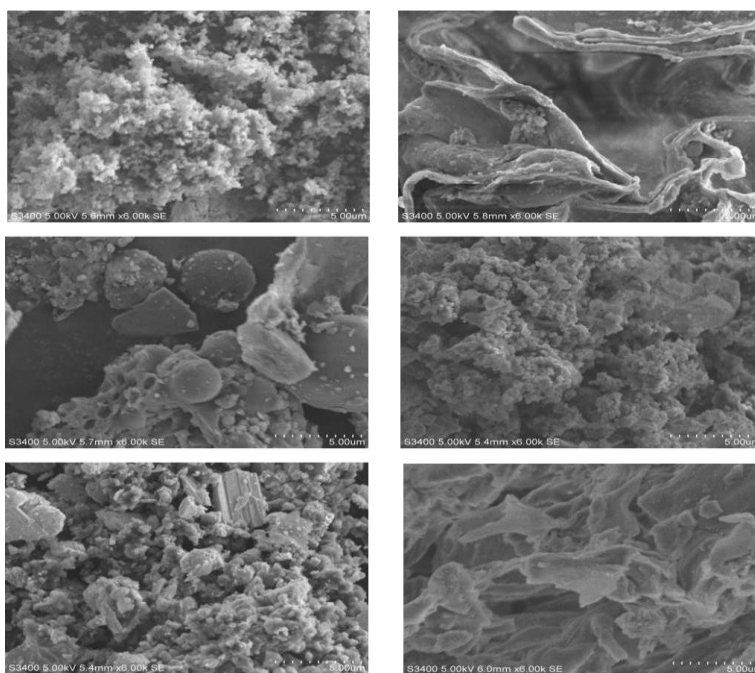


**Figure-2: SEM image of PANI and Composite**

### 5.3 FTIR :

Figure-3 shows the FTIR of PPy-PbO composites with different wt%. S-O Bonding Interaction: A characteristic absorption band at  $1041.65\text{ cm}^{-1}$  indicates the presence of S-O bonding interaction between PPy and PbO. This peak suggests that there is a chemical interaction between sulfur (S) from PPy and oxygen (O) from PbO.



Absorption peaks at  $896.80\text{ cm}^{-1}$ ,  $771.8\text{ cm}^{-1}$ ,  $772.280\text{ cm}^{-1}$ ,  $785.8\text{ cm}^{-1}$ , and  $774.10\text{ cm}^{-1}$  are attributed to C-C bonds in the aromatic rings of PPy. These peaks indicate the presence of the carbon-carbon bonding within the PPy structure.

Peaks at  $2661.97\text{ cm}^{-1}$ ,  $2675.39\text{ cm}^{-1}$ ,  $2734.37\text{ cm}^{-1}$ , and  $2685.74\text{ cm}^{-1}$  are due to the formation of hydrogen bonding (H-bonding) and interactions between PPy and PbO.

These peaks suggest interactions between the hydrogen (H) atoms in PPy and the oxygen (O) atoms in PbO, indicating a chemical interaction between the two components.

The FTIR spectra show that the addition of PbO to PPy results in shifts in the absorption peaks. These shifts are observed at specific wavenumbers and indicate changes in chemical bonding and interactions.

The shift from  $1041.64\text{ cm}^{-1}$  to  $1550.77\text{ cm}^{-1}$  suggests a change in the S-O bonding interaction when PbO is added. Similarly, shifts in other peaks like  $2675.38\text{ cm}^{-1}$  to  $2734.36\text{ cm}^{-1}$  and  $774.11\text{ cm}^{-1}$  to  $785.89\text{ cm}^{-1}$  indicate changes in H-bonding and C-C bonding interactions. The FTIR data also suggest that there is interaction between the N-H group of PPy and the surface of PbO. This interaction results in shifts in the peaks associated with C-N and C-C bonds toward higher frequencies.

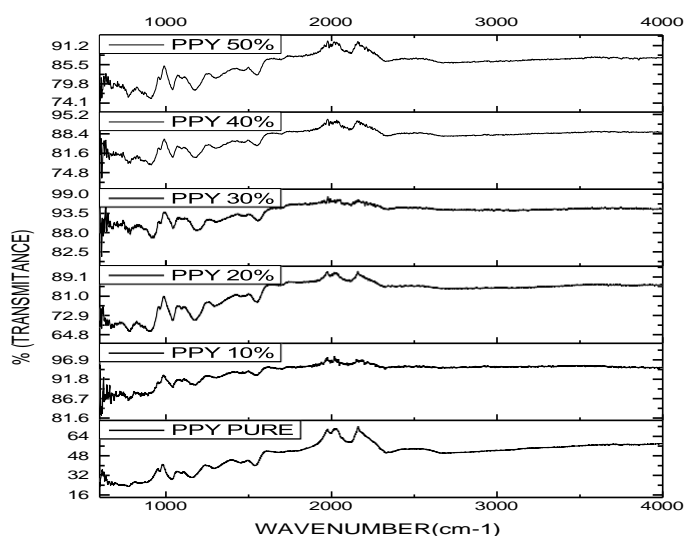


**Figure-3:** FTIR spectra of PPy-PbO composites with different wt%

#### 5.4 TGA and DTA analysis:

TGA of PPy and PbO nanocomposite materials in nitrogen and oxygen atmosphere at 60% RH are observed from the figure 4,

Thermal stability of PbO is observed to be significantly higher than that of pure PPy in the temperature range of 30-600°C. This suggests that PbO contributes to enhancing the overall thermal stability of the nanocomposite. PPy is described as hygroscopic, as it undergoes a weight loss of approximately 7.9 wt% at 200°C due to the evaporation of water absorbed by the material.

The PPy-PbO nanocomposite exhibits a much lower weight loss (only 2 wt%) at 200°C, indicating reduced water content. As the temperature increases, weight loss occurs in the PPy-PbO nanocomposite at around 450°C. This is likely associated with thermal decomposition or other processes within the composite.

Pure PPy, on the other hand, experiences a significant weight loss starting at 288°C and continuing until 534°C.

Differential Thermal Analysis (DTA) conducted under N<sub>2</sub> atmosphere for PPy shows an endothermic peak at 460.5°C, which could be indicative of a thermal transition or reaction.

Under O<sub>2</sub> atmosphere, PPy exhibits a sharp exothermic peak at the same temperature (460.5°C), suggesting that additional oxygen is involved in the reaction. The data indicates that the presence of PbO in the PPy-PbO nanocomposite has an impact on the thermal stability of the material. The exothermic peaks observed in the nanocomposite move to higher temperatures, indicating increased thermal stability and orderliness of PPy chains within the composite.

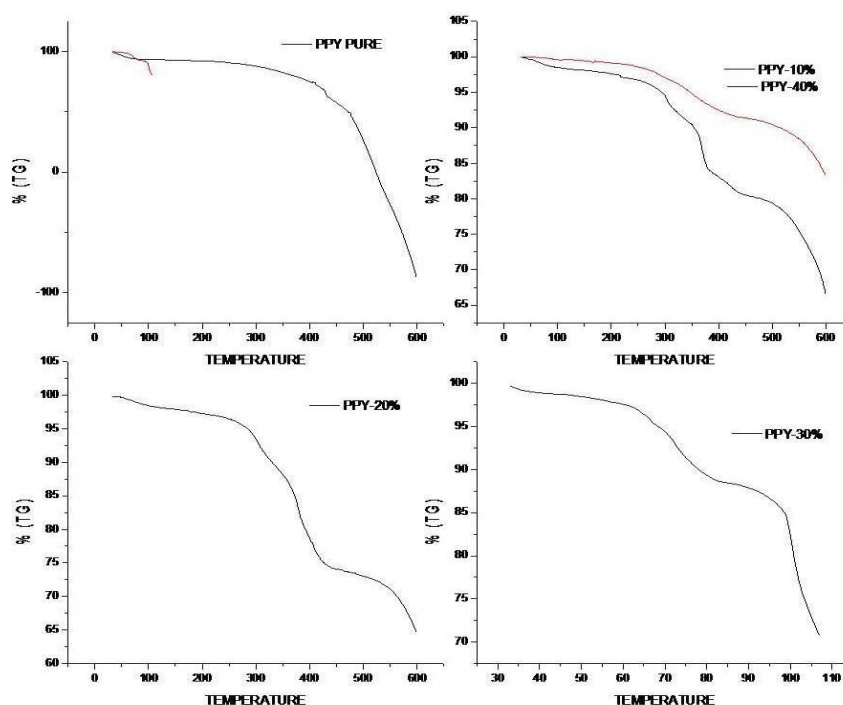


Figure-4: Thermal gravimetric analysis of PPy and PbO

## 6. Conclusion:

SEM micrographs demonstrate the complete encapsulation of PbO particles within the PPy matrix. The grains exhibit spherical morphology with an average particle size of around 10  $\mu\text{m}$ . The addition of PbO to PPy significantly affects the morphology, resulting in irregularly shaped particles with agglomeration. Varied development of crystalline nature is observed in some regions of the composite. The FTIR analysis reveals various characteristic absorption bands: S-O bonding interaction between PPy and PbO at 1041.65  $\text{cm}^{-1}$ .

C-C bonds in the aromatic ring at  $896.80\text{ cm}^{-1}$ ,  $771.81\text{ cm}^{-1}$ ,  $772.28\text{ cm}^{-1}$ ,  $785.90\text{ cm}^{-1}$ , and  $774.11\text{ cm}^{-1}$ . Interaction between PPy-PbO via H-bonding at peaks like  $2661.98\text{ cm}^{-1}$ ,  $2675.39\text{ cm}^{-1}$ ,  $2734.37\text{ cm}^{-1}$ , and  $2685.\text{ cm}^{-1}$ . Interaction of H-N band with oxygen from PbO.

The XRD pattern of pure PPy indicates amorphous nature, with no Bragg's reflection, the composite exhibits Bragg's reflections, indicating the development of crystallinity within the PPy-PbO nanocomposite. The average crystallite size of the composite is calculated to be 3 nm.

TGA shows that PbO has significantly higher thermal stability compared to PPy. PPy is hygroscopic and experiences a weight loss of approximately 7.9 wt% at  $200^{\circ}\text{C}$  due to water evaporation. The PPy-PbO nanocomposite exhibits reduced water evaporation (only 2 wt% loss at  $200^{\circ}\text{C}$ ). Weight loss in the nanocomposite occurs at higher temperatures (around  $450^{\circ}\text{C}$ ) compared to PPy (starting at  $288^{\circ}\text{C}$ ). The presence of PbO enhances the thermal stability of the composite.

## 7. References:

- [1] S. C. Rasmussen, "The Early History of Polyaniline: Discovery and Origins," *An Int. J. Hist. Chem. Subst.*, vol. 1, no. 12, pp. 99–109, 2017, doi: 10.13128/substantia-30.
- [2] S. M. Pethe and S. B. Kondawar, "Optical and electrical properties of conducting polyaniline nanofibers synthesized by interfacial and rapid mixing polymerization," *Adv. Mater. Lett.*, vol. 5, no. 12, pp. 728–733, 2014, doi: 10.5185/amlett.2014.amwc550.
- [3] T. Sen, S. Mishra, and N. G. Shimpi, "Synthesis and sensing applications of polyaniline nanocomposites: A review," *RSC Adv.*, vol. 6, no. 48, pp. 42196–42222, 2016, doi: 10.1039/c6ra03049a.
- [4] I. Rahayu et al., "The effect of hydrochloric acid-doped polyaniline to enhance the conductivity," in *IOP Conference Series: Materials Science and Engineering*, May 2019, vol. 509, no. 1, doi: 10.1088/1757-899X/509/1/012051.
- [5] A. G. MacDiarmid, "'Synthetic metals': A novel role for organic polymers (Nobel lecture)," *Angewandte Chemie - International Edition*, vol. 40, no. 14, pp. 2581–2590, 2001, doi: 10.1002/1521-3773(20010716)40:14<2581:AID-ANIE2581>3.0.CO;2-2.
- [6] K. Crowley, M. R. Smyth, A. J. Killard, and A. Morrin, "Printing polyaniline for sensor applications," *Chemical Papers*, vol. 67, no. 8, pp. 771–780, 2013, doi: 10.2478/s11696-0120301-9.
- [7] AL-Mokaram, A.M.A.A., Yahya, R., Abdi, M.M. and Mahmud, H.N.M.E. "One-step electrochemical deposition of Polypyrrole–Chitosan–Iron oxide nanocomposite films for non- enzymatic glucose biosensor," *Materials Letters*, vol.183, pp.90-93,2016, doi: 10.1016/j.matlet.2016.07.049.
- [8] M. Mozafari and N. P. S. Chauhan, "Fundamentals and emerging applications of polyaniline," *Fundam. Emerg. Appl. Polyaniline*, pp. 1–308, 2019, doi: 10.1016/C2018-0-027073.
- [9] S. Virji et al., "Construction of a polyaniline nanofiber gas sensor," *J. Chem. Educ.*, vol. 85, no. 8, pp. 1102–1104, 2008, doi: 10.1021/ed085p1102.
- [10] J. Huang, S. Virji, B. H. Weiller, and R. B. Kaner, "Nanostructured Polyaniline Sensors," *Chemistry - A European Journal*, vol. 10, no. 6, pp. 1314–1319, 2004, doi: 10.1002/chem.200305211.





- 
- [11] P. P. Sengupta, S. Barik, and B. Adhikari, "Polyaniline as a gas-sensor material," *Mater. Manuf. Process.*, vol. 21, no. 3, pp. 263–270, 2006, doi: 10.1080/10426910500464602.
- [12] F. W. Zeng, X. X. Liu, D. Diamond, and K. T. Lau, "Humidity sensors based on polyaniline nanofibres," *Sensors Actuators, B Chem.*, vol. 143, no. 2, pp. 530–534, 2010, doi: 10.1016/j.snb.2009.09.050.
- [13] J. S. Do and S. H. Wang, "On the sensitivity of conductimetric acetone gas sensor based on polypyrrole and polyaniline conducting polymers," *Sensors Actuators, B Chem.*, vol. 185, pp. 39–46, 2013, doi: 10.1016/j.snb.2013.04.080.
- [14] K. M. Polizzi, "Biosensors," in *Comprehensive Biotechnology*, 2019, pp. 572–584.
- [15] S. Majumder, T. Mondal, and M. J. Deen, "Wearable sensors for remote health monitoring," *Sensors (Switzerland)*, vol. 17, no. 1. 2017, doi: 10.3390/s17010130.
- [16] M. Zhybak, V. Beni, M. Y. Vagin, E. Dempsey, A. P. F. Turner, and Y. Korpan, "Creatinine and urea biosensors based on a novel ammonium ion-selective copper-polyaniline nano-composite," *Biosens. Bioelectron.*, vol. 77, pp. 505–511, 2016, doi:10.1016/j.bios.2015.10.009.